2D Materials through the lens of

X-ray absorption spectroscopies

Adriana I. Figueroa
Condensed Matter Physics Department and Institute of Nanoscience and Nanotechnology
University of Barcelona, Spain

Synchrotron Radiation

Naturally focused towards the forward direction

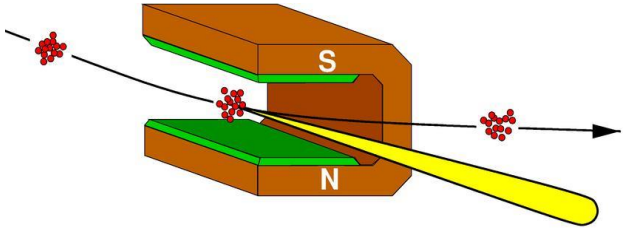

Wide spectral range: from IR to γ-rays

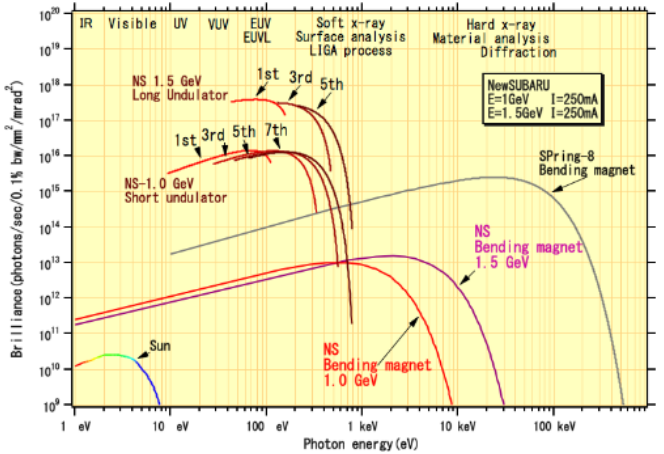

Pulsed time-structure

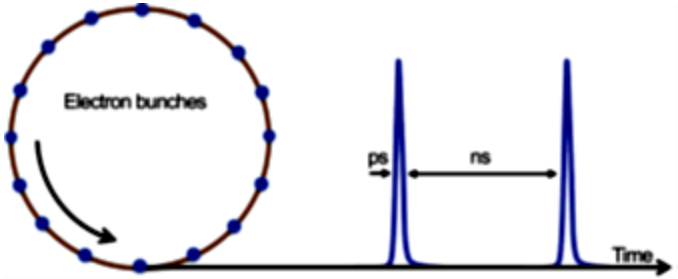

Horizontally polarized on the orbital plane

Radiation-Matter interaction

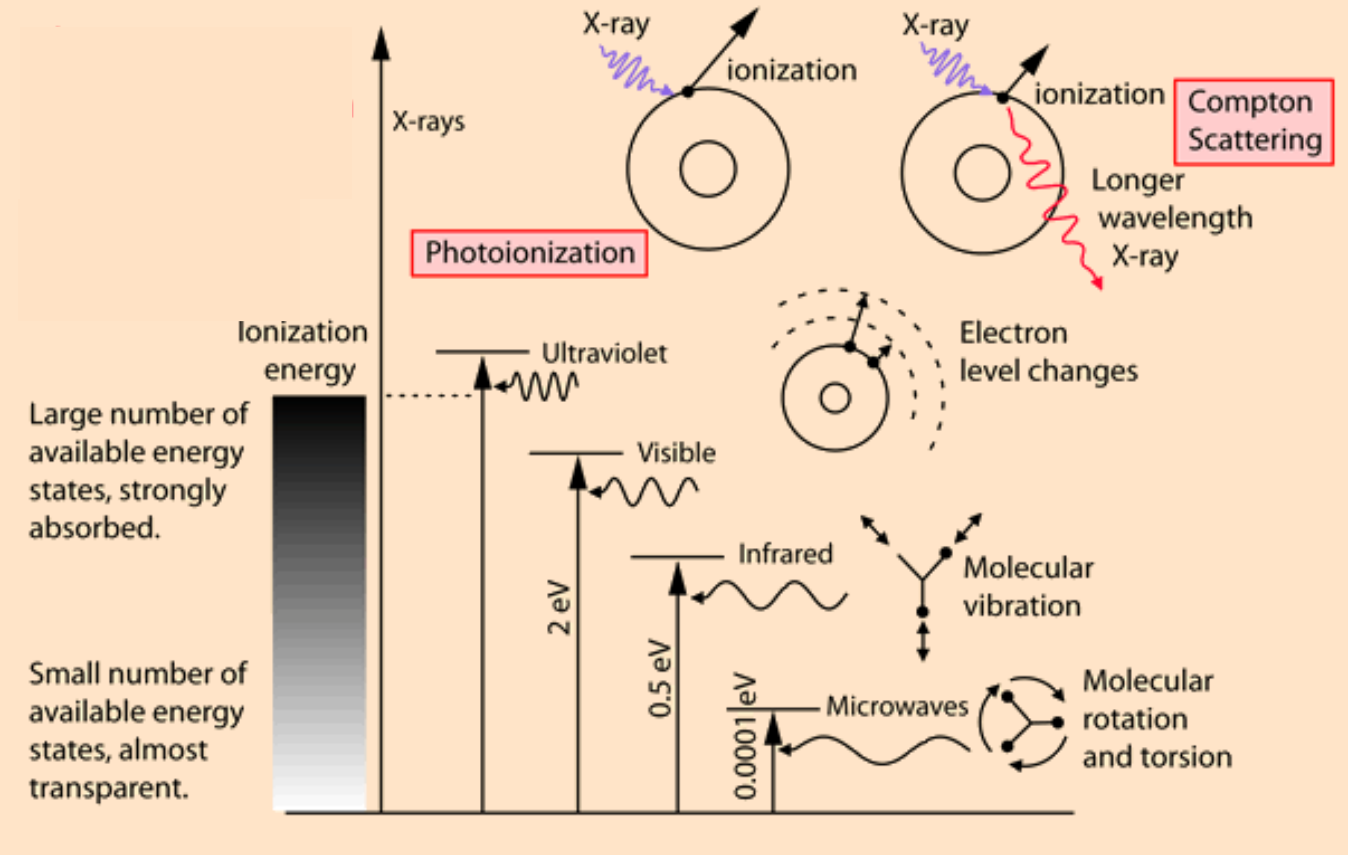

http://hyperphysics.phy-astr.gsu.edu/hbase/mod3.html

Radiation-Matter interaction: X-rays & γ-rays

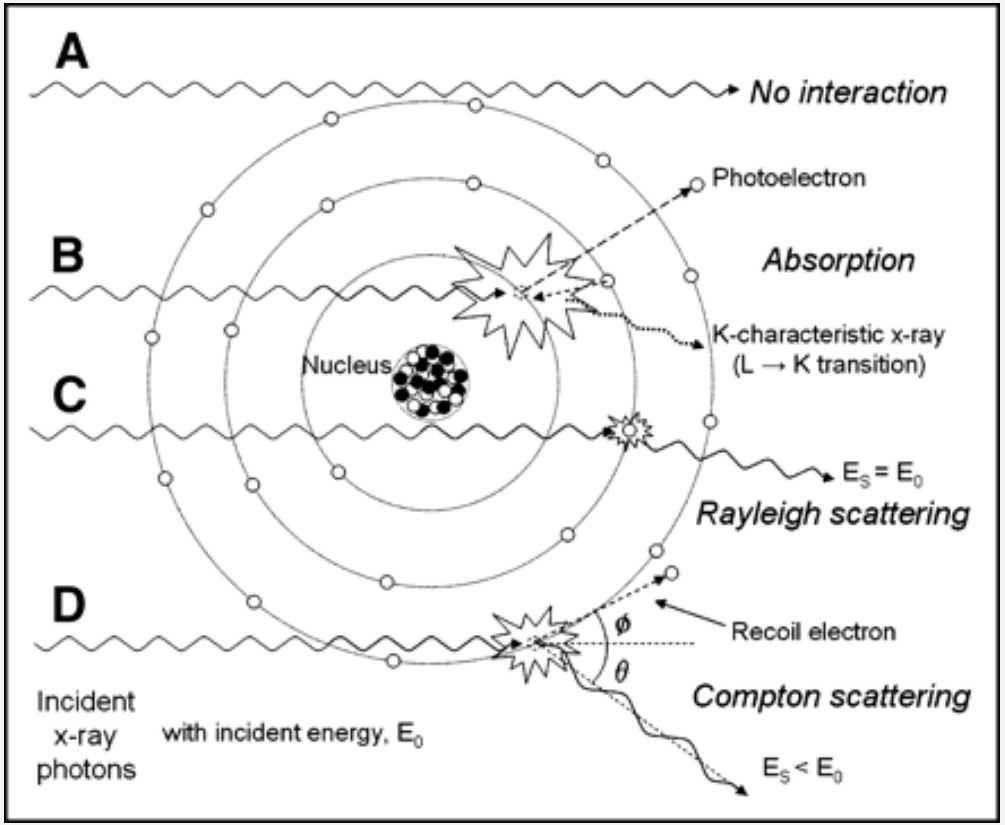

J. Nucl. Med. Technol. 33 (1) 3-18 (2005)

Synchrotron Radiaton Techniques

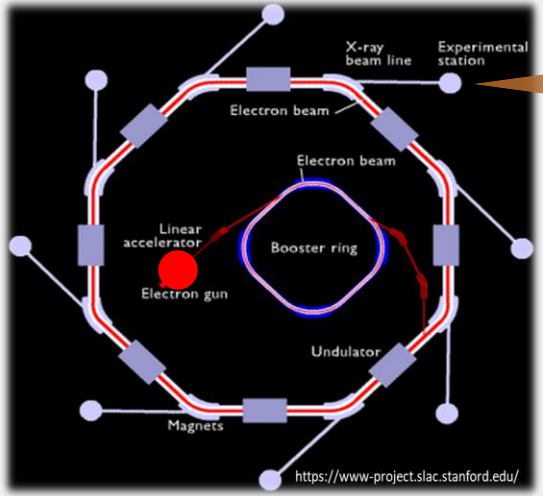

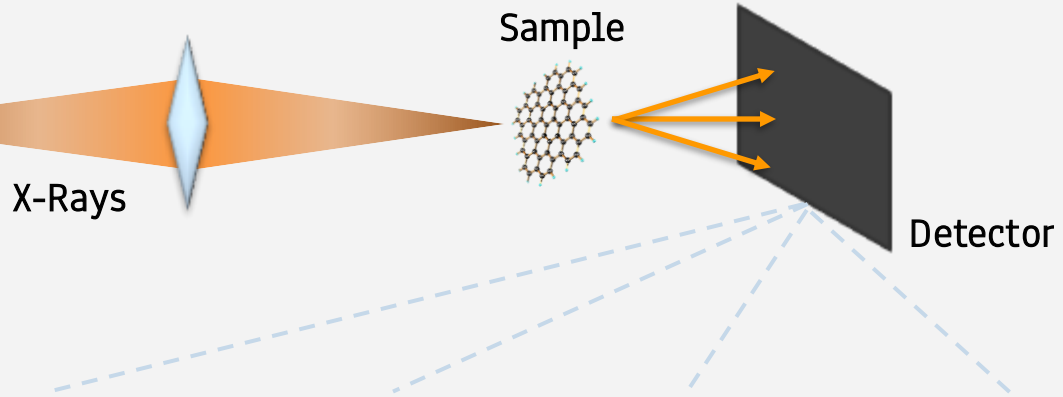

Energy	Momentum	Positon	Dynamics
Spectroscopy	**Scattering**	**Imaging**	**Time-resolving**
XAS	XRD	Microscopy	Diffraction
Fluorescence	SAXS	Tomography	Luminescence
Spectromicroscopy	XRMS	Phasing	Spectroscopy
	RIXS	Litography	Imaging

https://photon-science.desy.de/research/students__teaching/primers/experimental_techniques/index_eng.html

X-ray Absorption Spectroscopy (XAS)

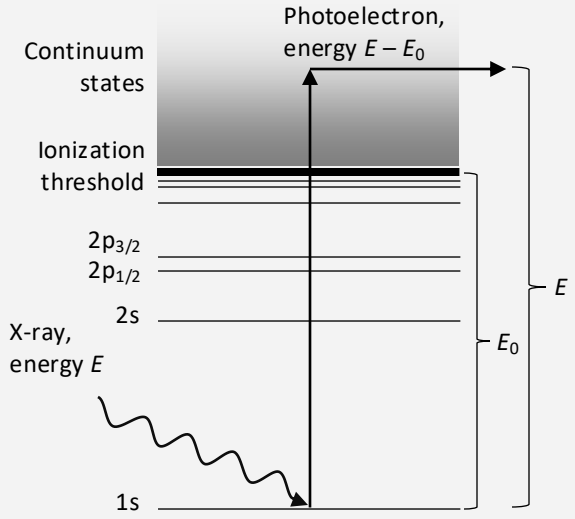

At the ***absorption edge***, the X-ray photon will have enough energy to promote the transition to the **unoccupied state**.

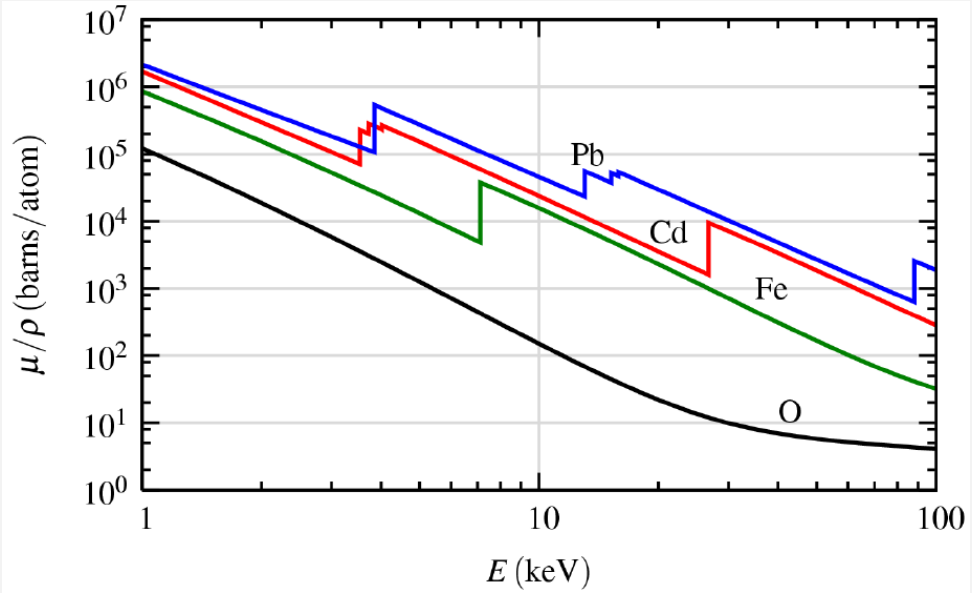

The energy position of the resonant spectra (binding energy) depends strongly on the nuclear charge

Element Specific

M. Newville, Fundamentals of XAFS, Rev. Miner. and Geochem. **78** (2014), 33-74

X-ray Absorption Spectroscopy (XAS)

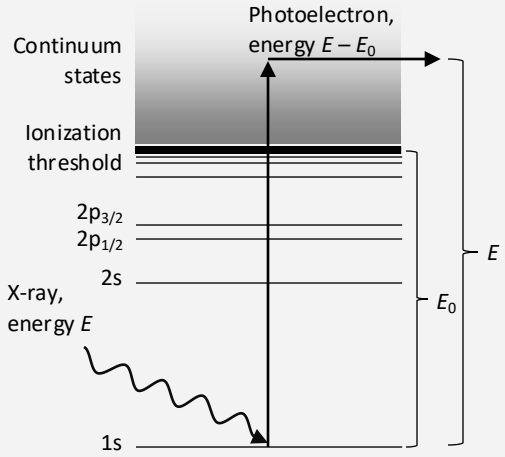

If the energy is large enough, the electron is ejected from the atom: photoelectric effect.

When reaching the continuum, it will **scatter with the neighbouring atoms** surrounding the absorbing atom

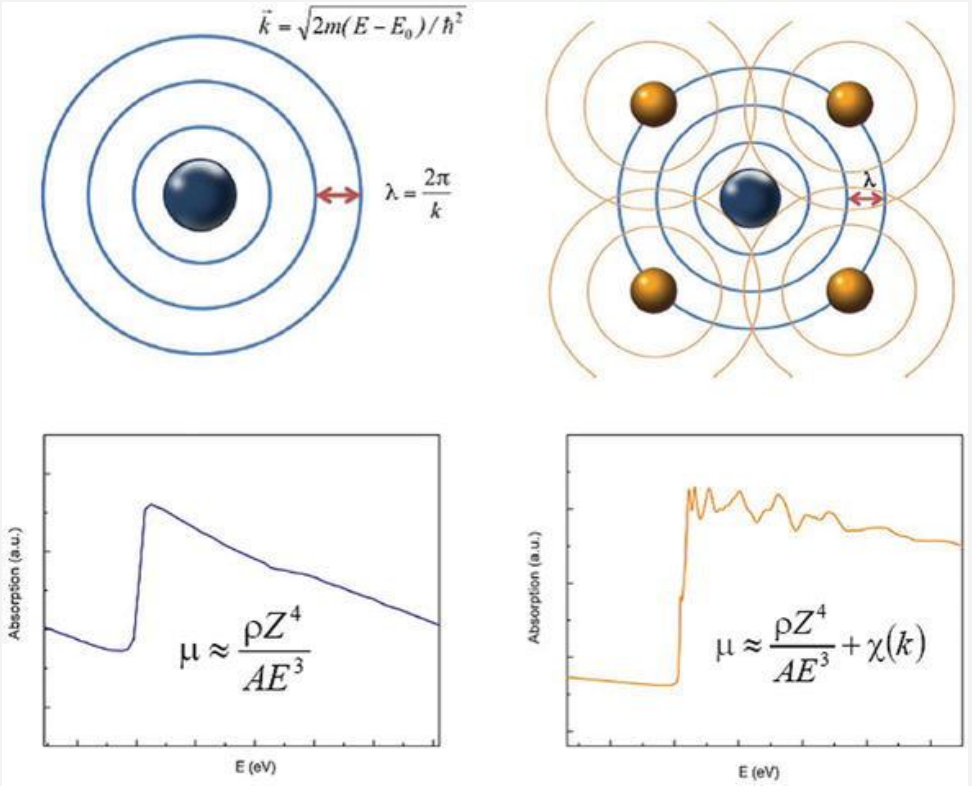

M. Newville, Fundamentals of XAFS, Rev. Miner. and Geochem. **78** (2014), 33-74

XAS: Measurements

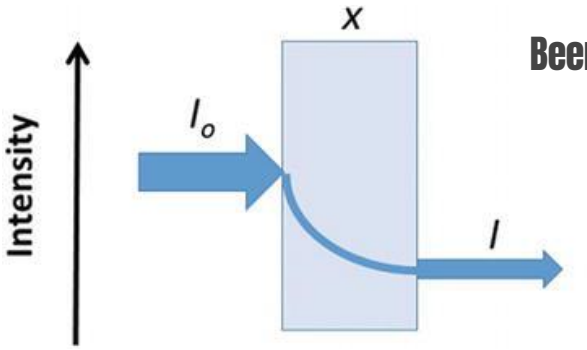

Beer-Lambert law

$$I = I_0 e^{-(\frac{\mu}{\rho})\rho x}$$

$$\mu \approx \frac{\rho Z^4}{AE^3}$$

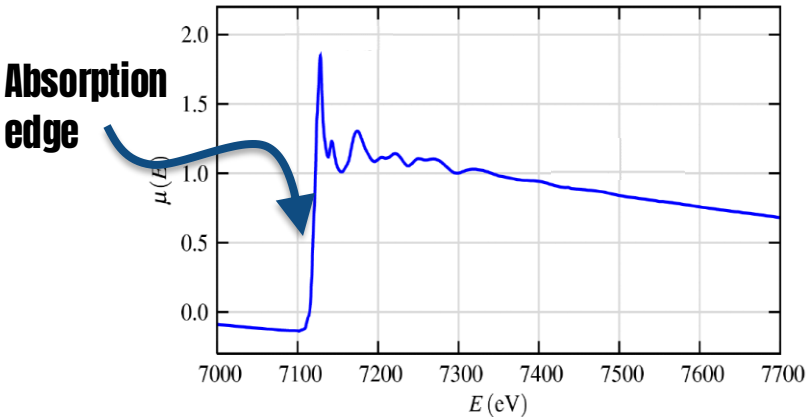

x: thickness of the material

μ: X-ray absorption coefficient

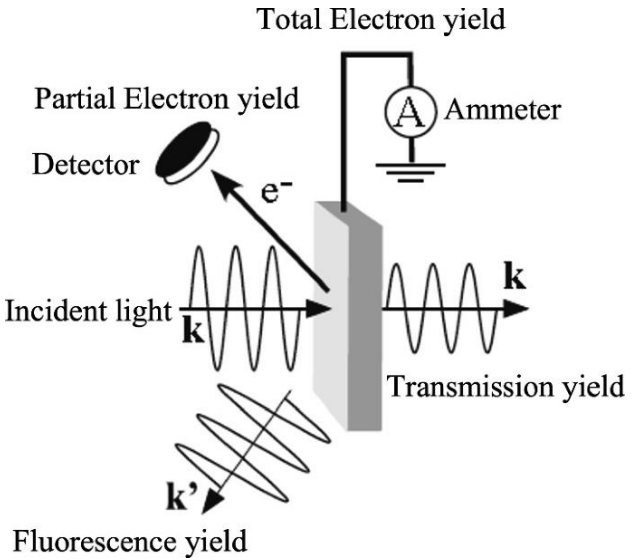

M. Newville, Fundamentals of XAFS, Rev. Miner. and Geochem. **78** (2014), 33-74

K (1s) and L_3 ($2p_{3/2}$) Electron Binding Energies for the Elements in Their Natural Forms, in eV

Legend: Element / K-edge / L_3-edge

H 13.6 n/a																	He 24.6 n/a
Li 54.7 n/a	Be 111.5 n/a											B 188 n/a	C 284.2 n/a	N 409.9 n/a	O 543.1 n/a	F 696.7 n/a	Ne 870.2 21.6
Na 1070.8 30.81	Mg 1303.0 49.50											Al 1559.6 72.55	Si 1839 99.42	P 2145.5 135	S 2472 162.5	Cl 2822 200	Ar 3205.9 248.5
K 3608.4 294.6	Ca 4038.5 346.2	Sc 4492 398.7	Ti 4966 453.8	V 5465 512.1	Cr 5989 574.1	Mn 6539 638.7	Fe 7112 706.8	Co 7709 778.1	Ni 8333 852.7	Cu 8979 932.7	Zn 9659 1021.8	Ga 10367 1116.4	Ge 11103 1217.0	As 11867 1323.6	Se 12658 1433.9	Br 13474 1550	Kr 14326 1678.4
Rb 15200 1804	Sr 16105 1940	Y 17038 2080	Zr 17998 2223	Nb 18986 2371	Mo 20000 2520	Tc 21044 2677	Ru 22117 2838	Rh 23220 3004	Pd 24350 3173	Ag 25514 3351	Cd 26711 3538	In 27940 3730	Sn 29200 3929	Sb 30491 4132	Te 31814 4341	I 33169 4557	Xe 34561 4786
Cs 35985 5012	Ba 37441 5247		Hf 65351 9561	Ta 67416 9881	W 69525 10207	Re 71676 10535	Os 73871 10871	Ir 76111 11215	Pt 78395 11546	Au 80725 11919	Hg 83102 12284	Tl 85530 12658	Pb 88005 13035	Bi 90524 13419	Po 93105 13814	At 95730 14214	Rn 98404 14619
Fr 101387 15031	Ra 103922 15444		Rf	Db	Sg	Bh	Hs	Mt	Ds	Rg	Cn	Uut	Uuq	Uup	Uuh	Uus	Uuo

La 38925 5483	Ce 40443 5723	Pr 41991 5964	Nd 43569 6208	Pm 45184 6459	Sm 46834 6716	Eu 48519 6977	Gd 50239 7243	Tb 51996 7514	Dy 53789 7790	Ho 55618 8071	Er 57486 8358	Tm 59390 8648	Yb 61332 8944	Lu 63314 9244
Ac 106768.2 15879.5	Th 109648.0 16300.0	Pa 112598.4 16732.9	U 115596.2 17164.7	Np 118688.7 17608.0	Pu 121790.2 18060.1	Am 124986.1 18510.0	Cm 128241.3 18970	Bk 131555.6 19449	Cf 134935.4 19901.2	Es 138391.5 20389.4	Fm 141930.4 20868.0	Md	No	Lr

J. A. Bearden and A. F. Burr, "Reevaluation of X-Ray Atomic Energy Levels," Rev. Mod. Phys. 39, 125 (1967)

M. Cardona and L. Ley, Eds., Photoemission in Solids I: General Principles (Springer-Verlag, Berlin, 1978)

J. C. Fuggle and N. Mårtensson, "Core-Level Binding Energies in Metals," J. Electron Spectrosc. Relat. Phenom. 21, 275 (1980)

Actinides (Ac-Fm): R.D. Deslattes, E.G. Kessler Jr., P. Indelicato, L. de Billy, E. Lindroth, J. Anton, J.S. Coursey, D.J. Schwab, J. Chang, R. Sukumar, K. Olsen, and R.A. Dragoset, "X-Ray Transition Energies Database", NIST Standard Reference Database 128, 2005; https://dx.doi.org/10.18434/T4859Z

X-ray Absorption Edges

	Cr	Mn	Fe	Co	Ni
K-edge	5989	6539	7112	7709	8333
L_3-edge	574.1	638.7	706.8	778.1	852.7

Edge		3*d* TM	4*d* TM	5*d* TM
K	$1s \rightarrow p$	5–11 keV	17–27 keV	65–81 keV
$L_{2,3}$	$2p \rightarrow d$	450–950 eV	2–4 keV	9–14 keV
$M_{2,3}$	$3p \rightarrow d$	30–125 eV	150–650 eV	1.7–3 keV
$N_{2,3}$	$4p \rightarrow d$	–	–	380–610 eV

G. van der Laan and AIF, Coord. Chem. Rev. **277**, 95 (2014)

Polarization dependent XAS

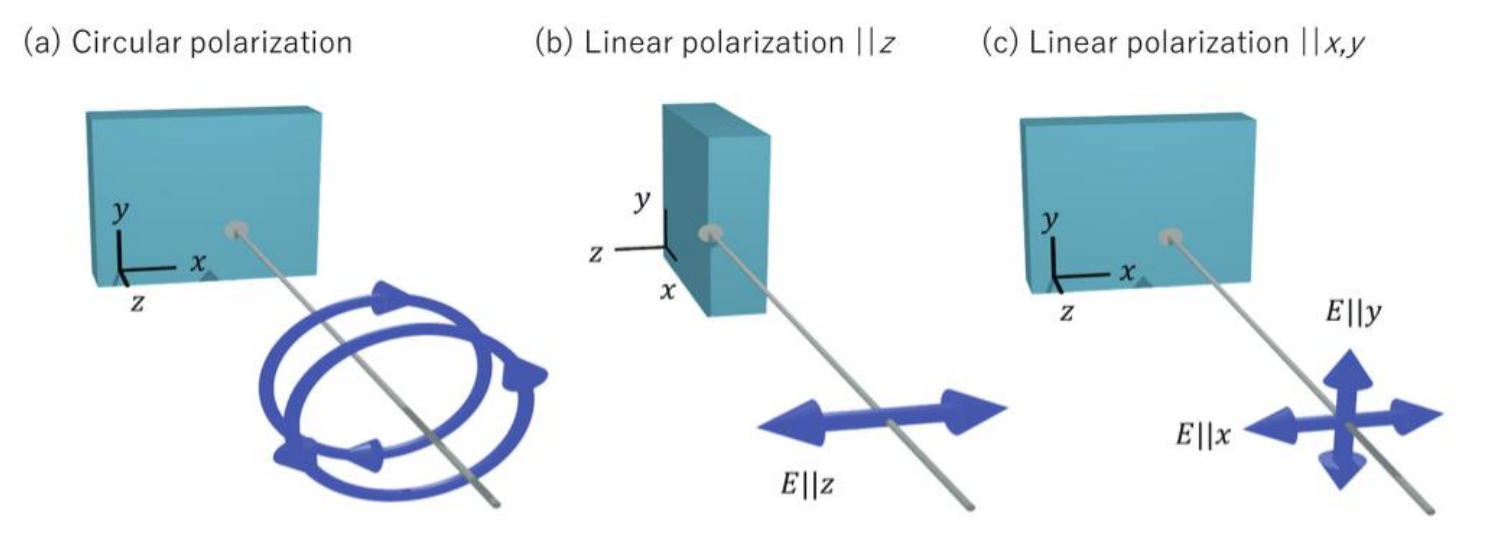

Y. Yamasaki. Science & Technology Of Advanced Materials 26, 1, 2513217 (2025)

X-ray Magnetic Circular Dichroism (XMCD)

difference in absorption for left- and right circularly polarized light.

$XMCD \propto \langle M_J \rangle$

X-ray Linear Dichroism (XMLD)

difference in absorption for linearly polarized light $\perp$ and // to quantization axis

$XMLD \propto \langle M_J^2 \rangle$

XMCD: magneto-optic effects

Hund's rules analysis for the ground state of a $3d^1$

L = 2 ; S = ½ and **J = L - S = 3/2**

For T → 0 and B → ∞ only m_J = -2 +1/2 = -3/2 is occupied (saturated)

Dipole-Selection-Rules: $\Delta J = \pm 1$ → circular Pol.: $\Delta m_J = \pm 1$

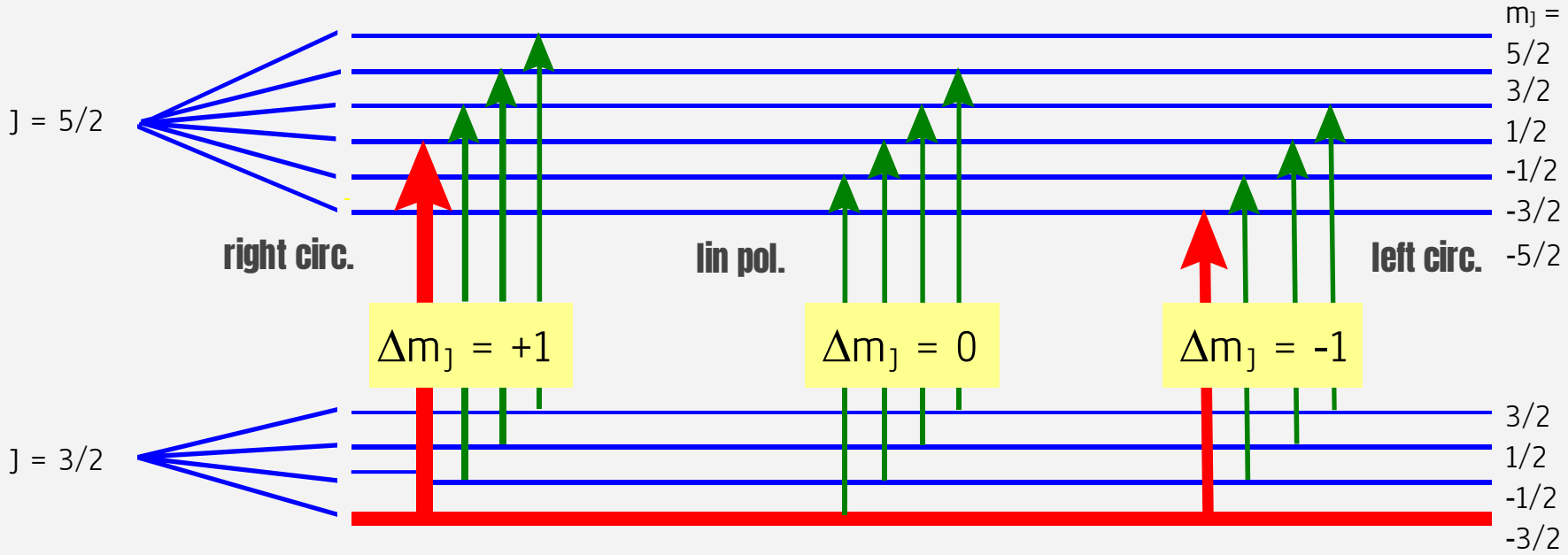

X-ray Magnetic Circular Dichroism (XMCD)

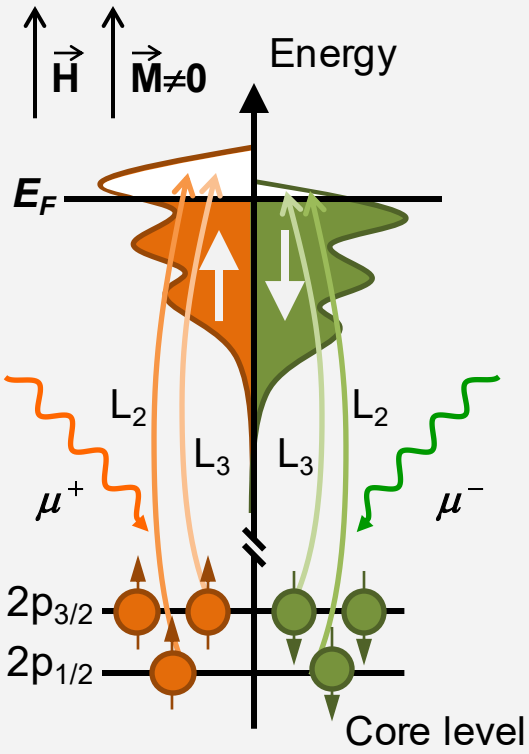

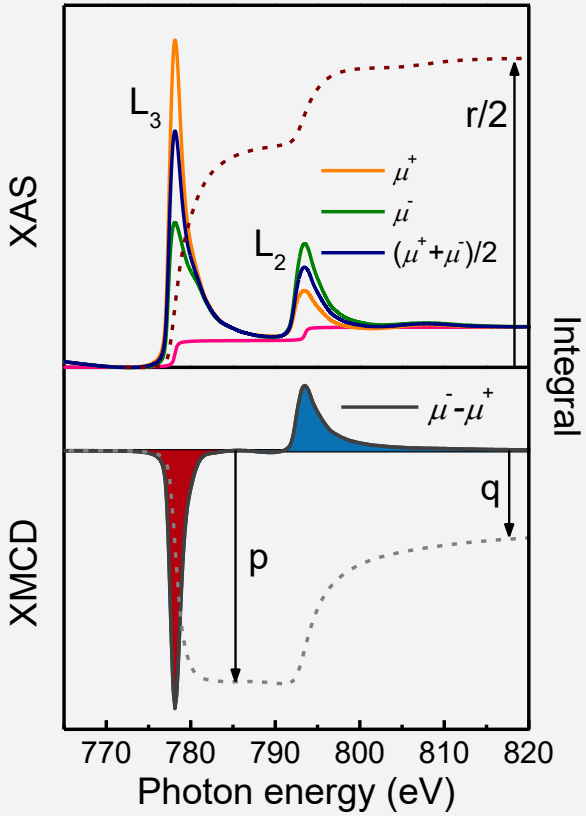

Magnetic sensitivity

- Spin-dependent absorption of circularly polarised photon
- Maximum when magnetization parallel to x-ray propagation
- Element, site and shell specific
- Application of sum rules allows for extraction of m_L and m_S

G. van der Laan and AIF, Coord. Chem. Rev. **277**, 95 (2014)

XMCD sum rules

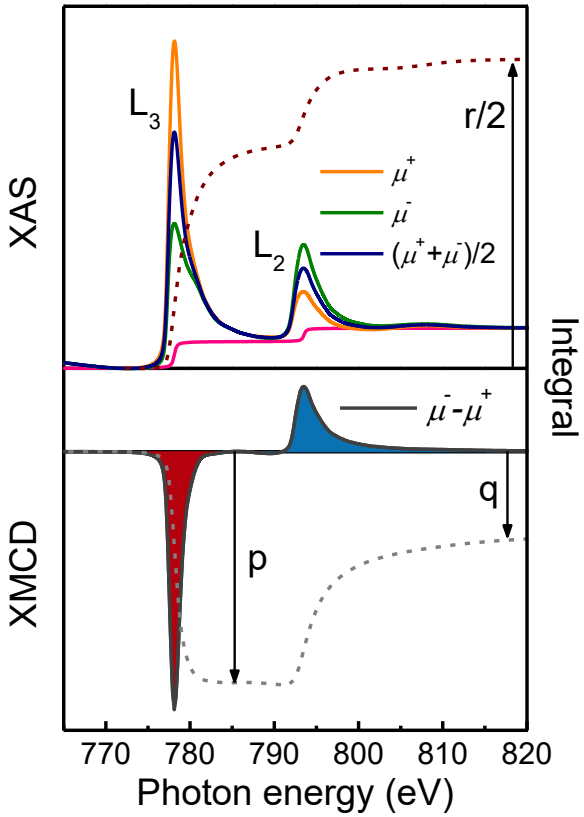

Branching ratio sum rule

$$B \equiv \frac{I(L_3)}{I(L_3)+I(L_2)} = B_0 + \frac{\langle \ell \cdot s \rangle}{n_h}$$

Orbital magnetic moment $$m_L = -\frac{4}{3}\frac{q}{r} n_h$$

Spin magnetic moment $$m_{S_{\text{eff}}} = -\frac{6p-4q}{r} n_h$$

Orbital to spin moment ratio $$\frac{m_L}{m_{S_{\text{eff}}}} = \frac{2}{3}\frac{q}{3p-2q}$$

B. T. Thole & G. van der Laan, Phys. Rev. B 38, 3158 (1988); B. T. Thole, et al. Phys. Rev. Lett. 68, 1943 (1992); P. Carra, et al. Phys. Rev. Lett. 70, 694 (1993); G. van der Laan, Phys. Rev. Lett. 82, 640 (1999)

XMCD sum rules

Contribution of L and S to XMCD signal

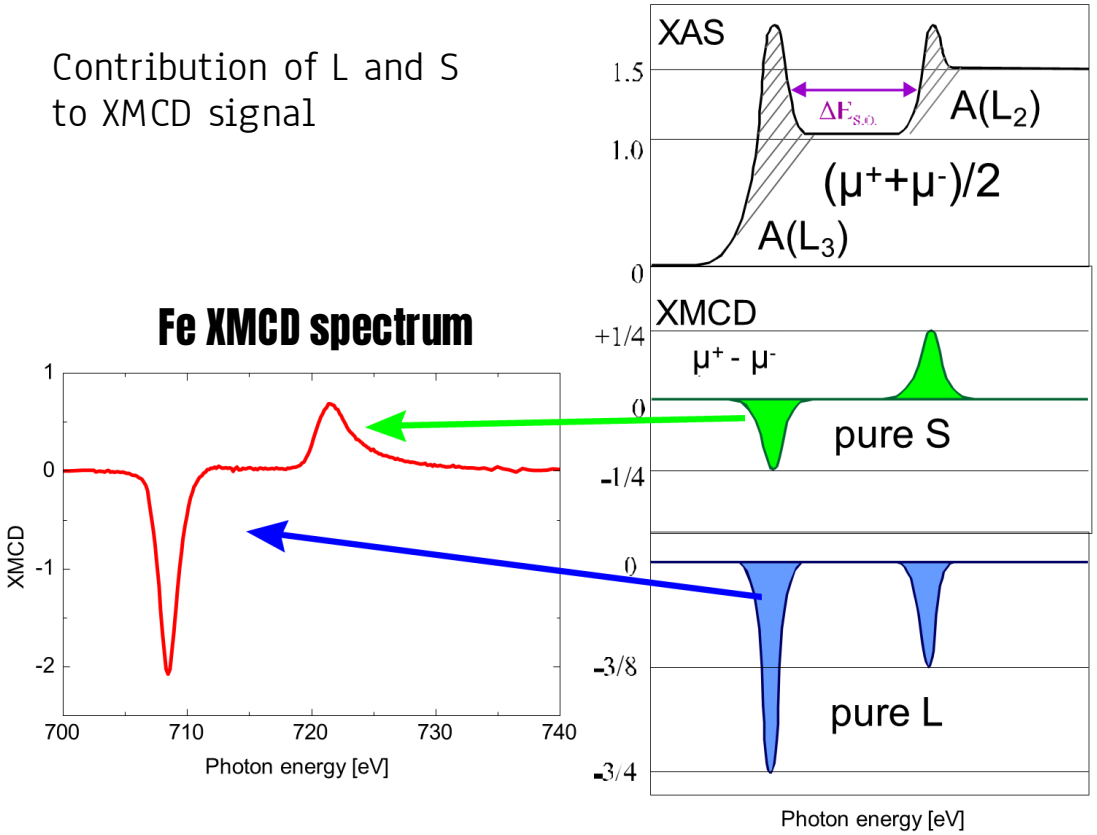

$$m_L = -\frac{4}{3}\frac{q}{r} n_h$$

$$m_{S_{\text{eff}}} = -\frac{6p - 4q}{r} n_h$$

$$\frac{m_L}{m_{S_{\text{eff}}}} = \frac{2}{3}\frac{q}{3p - 2q}$$

E. Goering, MPI-IS, Stuttgart. XMCD Lecture.

Example
XMCD on 2D magnets

An example of the use of XMCD to investigate the magnetism of Fe(Ge, Ga)Te family of 2D materials

2D Magnets

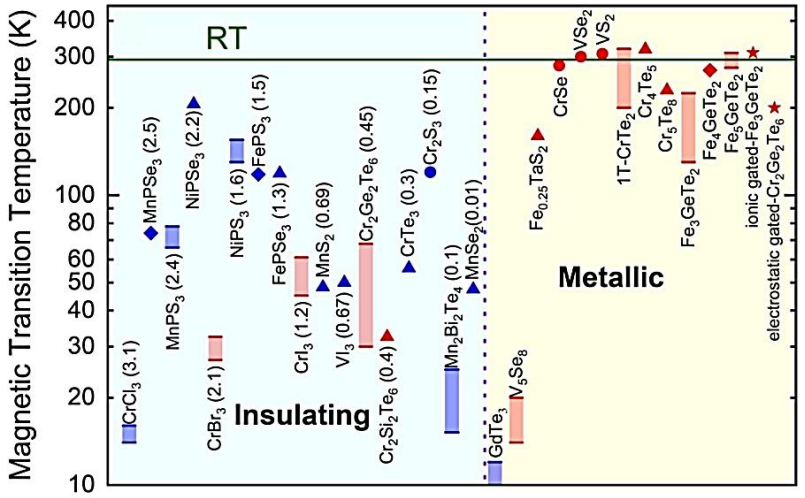

Kurebayashi et.al. Nat. Rev. **4**, 150 (2022)

Perpendicular magnetic anisotropy

Anisotropy-stabilized 2D magnetic order

Magnetism down to monolayer

Promising for ultra-compact spintronics

CrI_3

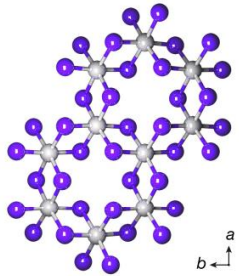

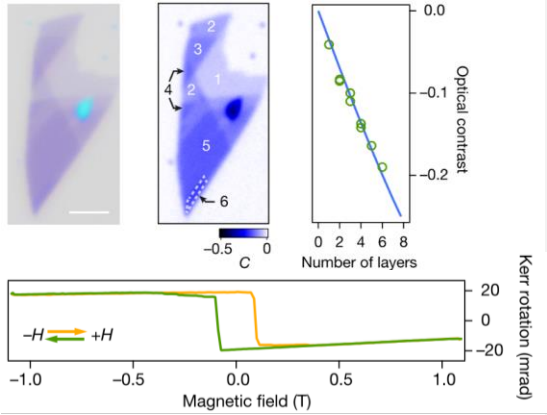

Huang et al. *Nature* **546**, 270 (2017)

Fe_3GeTe_2

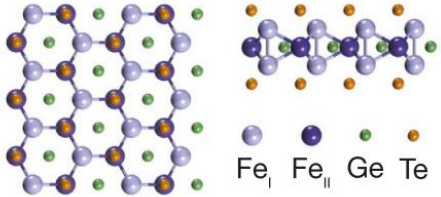

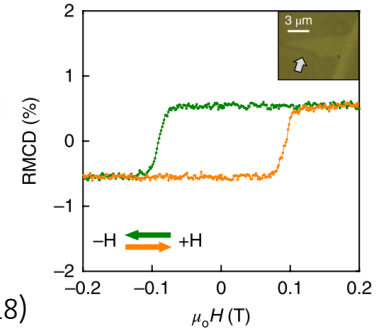

Fei et al., Nat. Mater. **17**, 778 (2018)

2D Magnets

Predicted family of half-metal 2D FM

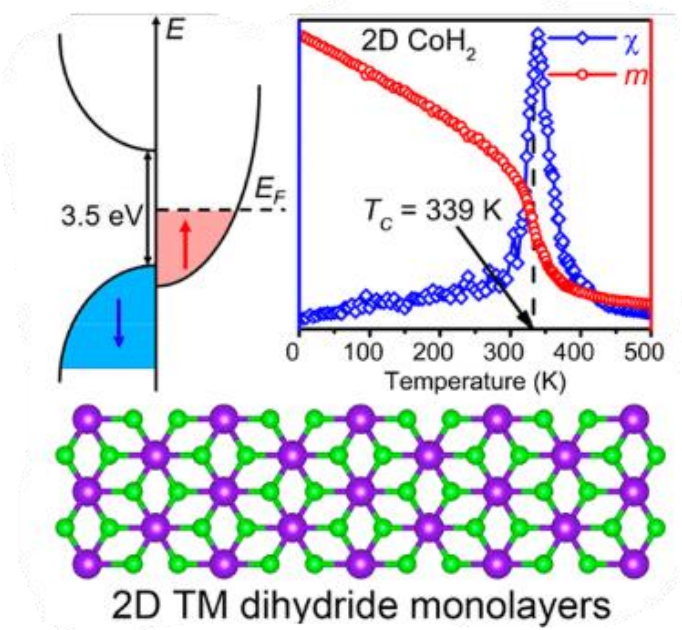

Q. Wu *et al.* J. Phys. Chem. Lett. 9 (2018) 15, 4260−4266

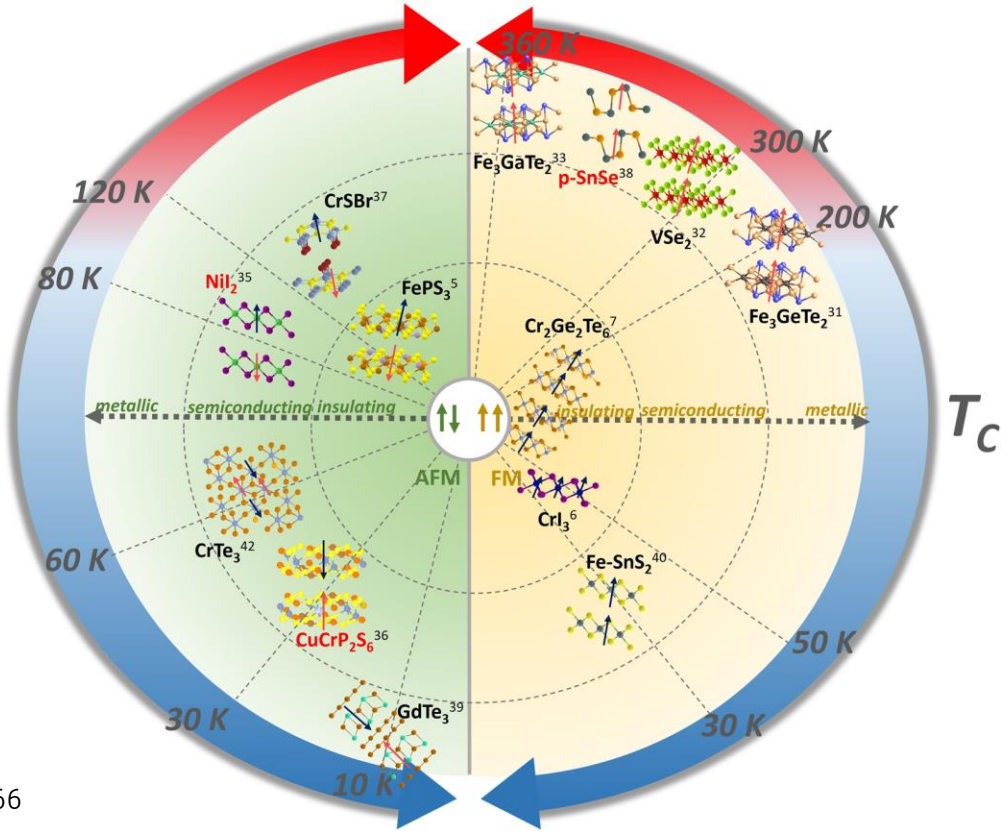

B. Zhang *et al.* npj Spintronics 2 (2024) 6

2D Magnets: The FeGeTe (FGT) family

- Metallic character: itinerant ferromagnetism
- High prospect for (above) room temperature operation
- Highly tunable properties

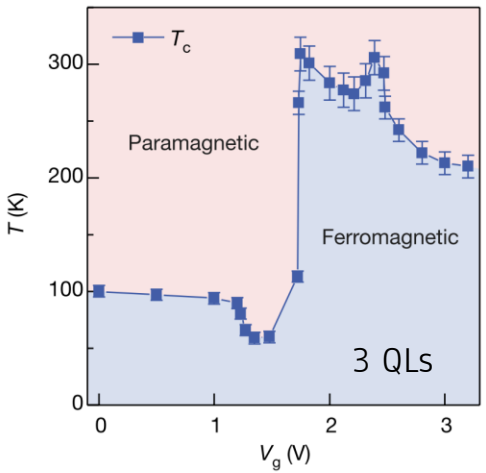

Deng et al., Nature **563**, 94 (2018)

Adding more Fe into FGT

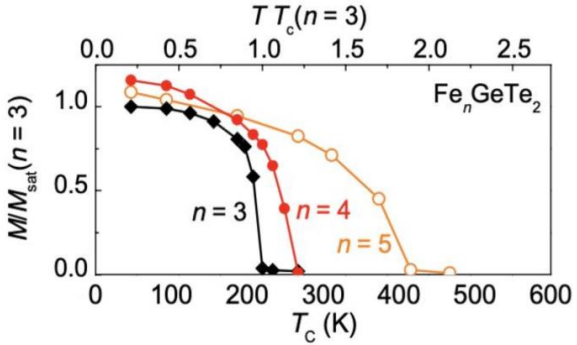

Seo et.al. *Sci. Adv.* **6**, eaay8912 (2020)

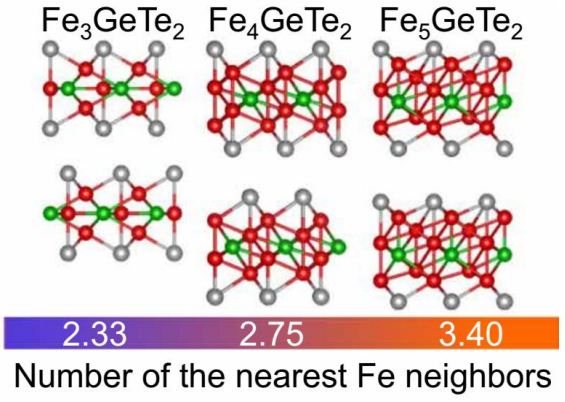

Control of T_C and anisotropy by Fe content, electrostatic gating, strain engineering …

Fe_3GeTe_2 on Gr/SiC

Magneto-transport

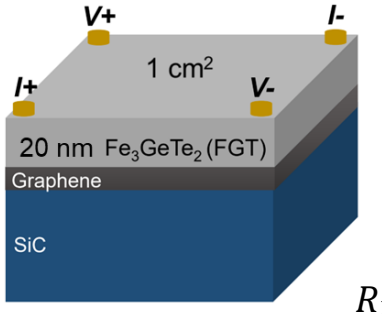

van der Pauw geometry

$$R_{XY} = R_{OHE} + R_{AHE}$$

$$R_{OHE} = \mu_0 R_O H$$

$$R_{AHE} = \mu_0 R_A M_z$$

Strong perpendicular magnetic anisotropy

Curie temperature around 220 K

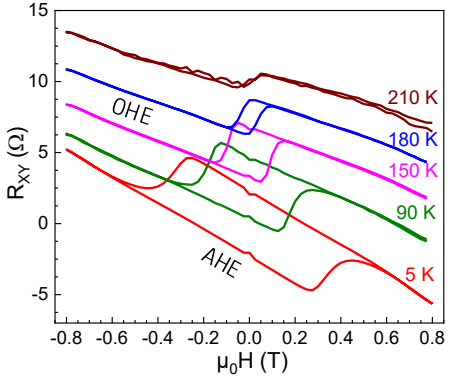

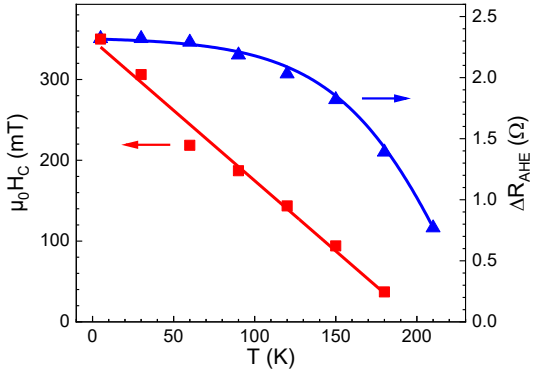

FGT Flakes

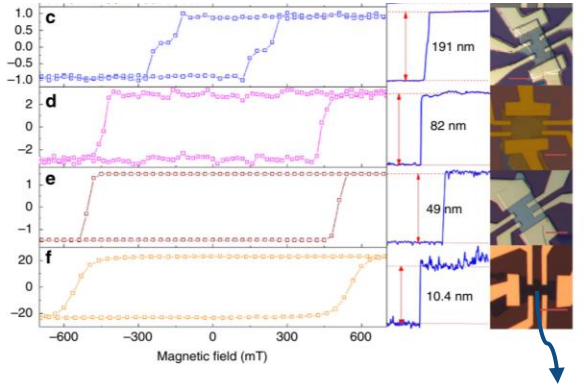

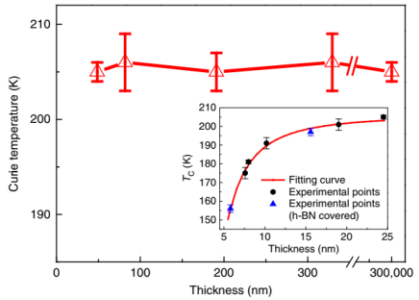

Lopes, … AIF, et al., 2D Materials **8**, 041001 (2021)

Tan et al., Nat. Comm. 9, 1554 (2018)

FGT on Gr/SiC: MBE growth

(1) Epitaxial graphene on SiC(0001)

- Si sublimation at 1600 °C in Ar/15 min
- Single- (SLG), Bi-(BLG) and few-layer graphene (FLG)
- Buffer layer (BL) on SiC(0001)

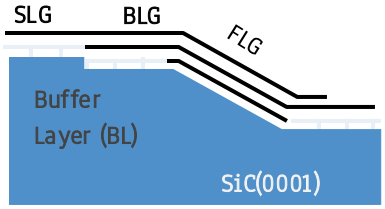

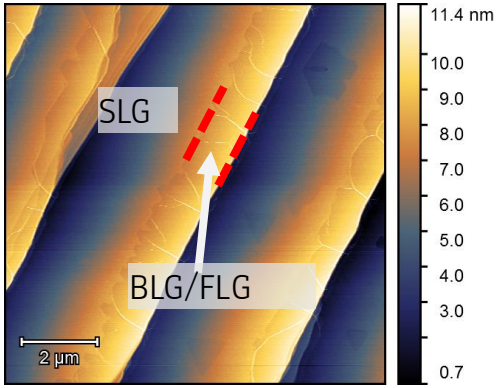

(2) MBE growth of $Fe_{5-x}GeTe_2$ (x = 2; 0)

- Growth temperature 300°C
- Fe:Ge:Te BEP* ratios: 1:1:20 (x ≈ 2)
  1.7:1:20 (x ≈ 0)
- Film thickness: 10nm to 20nm

* Beam equivalent pressure

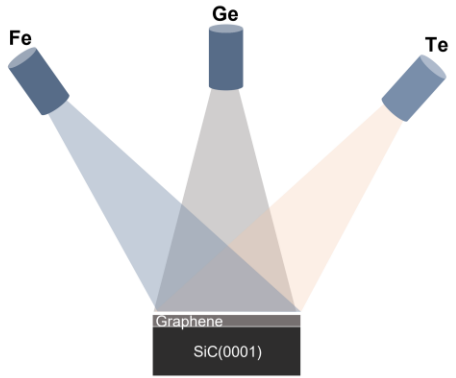

Lopes, … AIF, et al., 2D Materials **8**, 041001 (2021)

Fe_3GeTe_2 on Gr/SiC

Magneto-transport

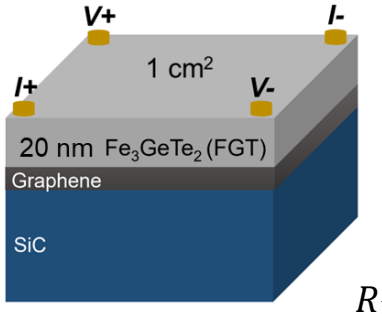

van der Pauw geometry

$$R_{XY} = R_{OHE} + R_{AHE}$$

$$R_{OHE} = \mu_0 R_O H$$

$$R_{AHE} = \mu_0 R_A M_z$$

Strong perpendicular magnetic anisotropy

Curie temperature around 220 K

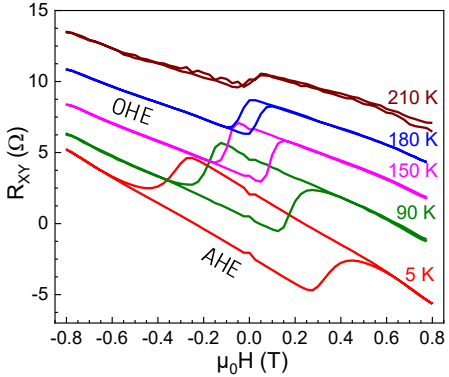

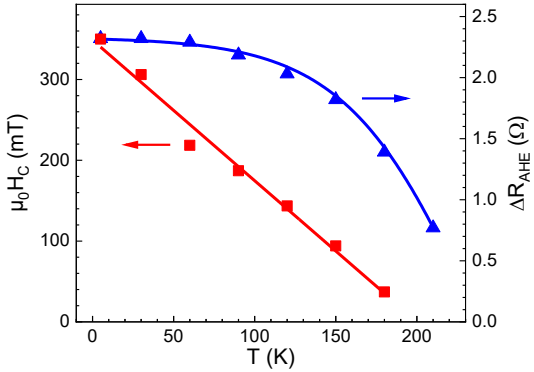

FGT Flakes

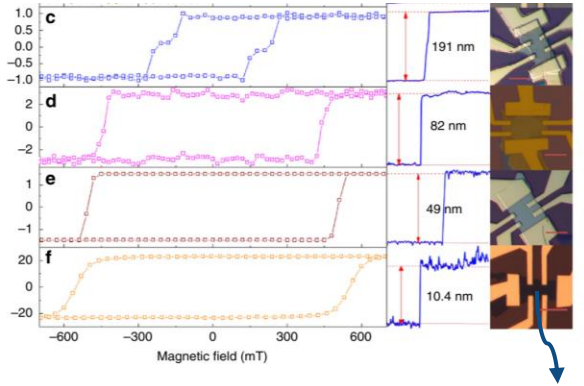

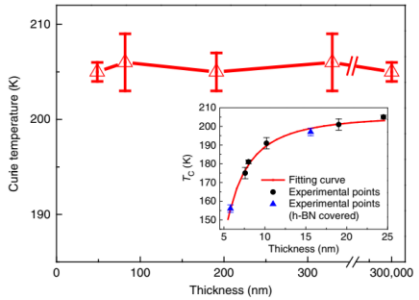

Lopes, ... AIF, et al., 2D Materials **8**, 041001 (2021)

Tan et al., Nat. Comm. 9, 1554 (2018)

Fe_3GeTe_2 on Gr/SiC

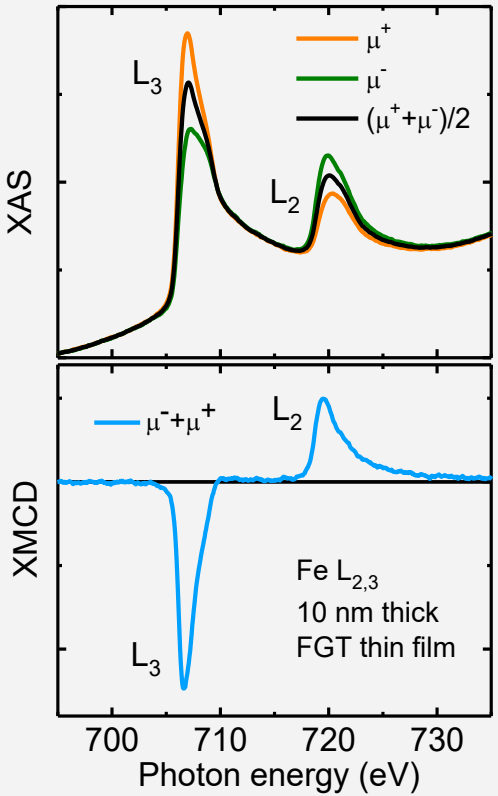

Microscopic magnetic properties by XMCD

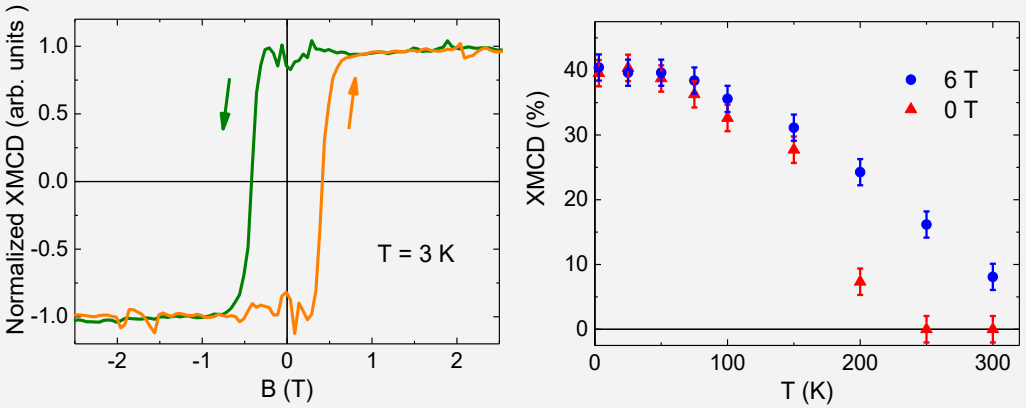

XMCD in agreement with magneto-transport results.

Application of sum rules yield magnetic moments:

μ_{Total} = 1.18 ± 0.10 μ_B /Fe

μ_{orb} = 0.047 ± 0.004 μ_B /Fe

μ_{spin} = 1.13 ± 0.09 μ_B/Fe

Lopes, … AIF, et al., 2D Materials 8, 041001 (2021)

$Fe_{4.75}GeTe_2$ on Gr/SiC

Magneto-transport

van der Pauw geometry

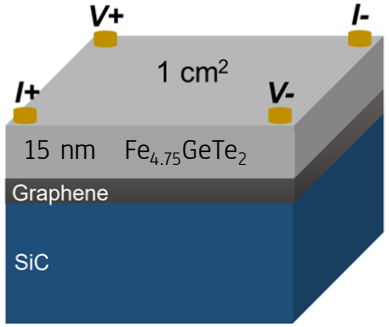

Ferromagnetism with out-of-plane remanence above room temperature

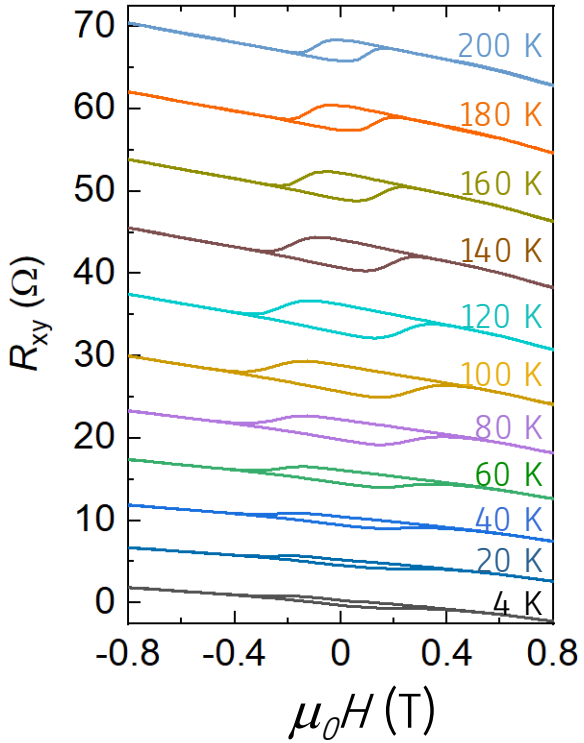

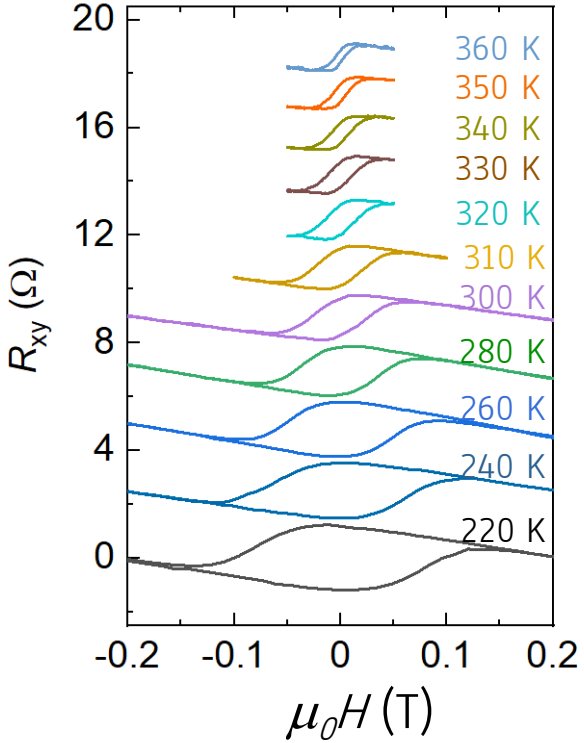

Lv, ... AIF, et al., Small 19, 2302387 (2023)

$Fe_{4.75}GeTe_2$ on Gr/SiC

Estimation of the Curie temperature, T_C from magneto-transport

Remanence of the AHE resistivity

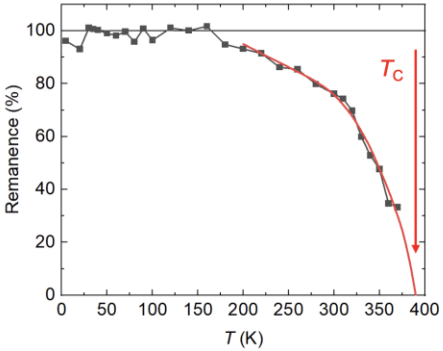

Coercivity

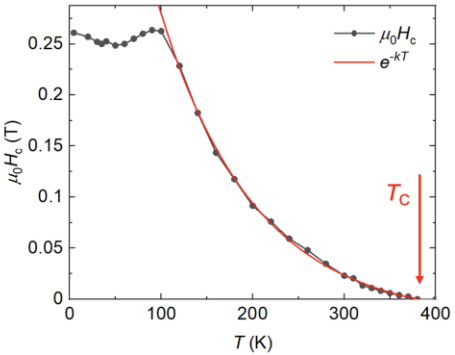

Arrott plot (ρ_A^2 vs. $\mu_0 H/\rho_A$)

ρ_A is the amplitude of an AHE hysteresis loop

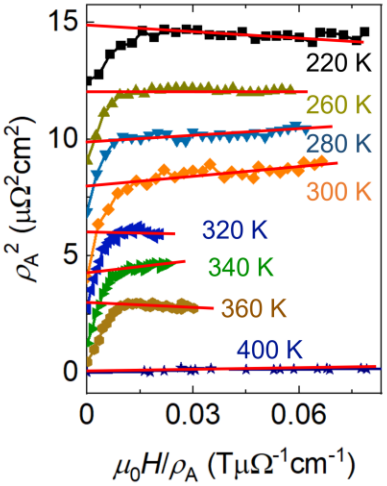

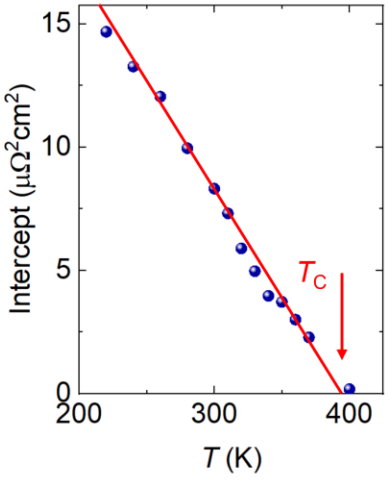

T_C above 350 K

Perpendicular magnetic anisotropy

Lv, ... AIF, et al., Small 19, 2302387 (2023)

$Fe_{4.75}GeTe_2$ on Gr/SiC

Estimation T_C from SQUID

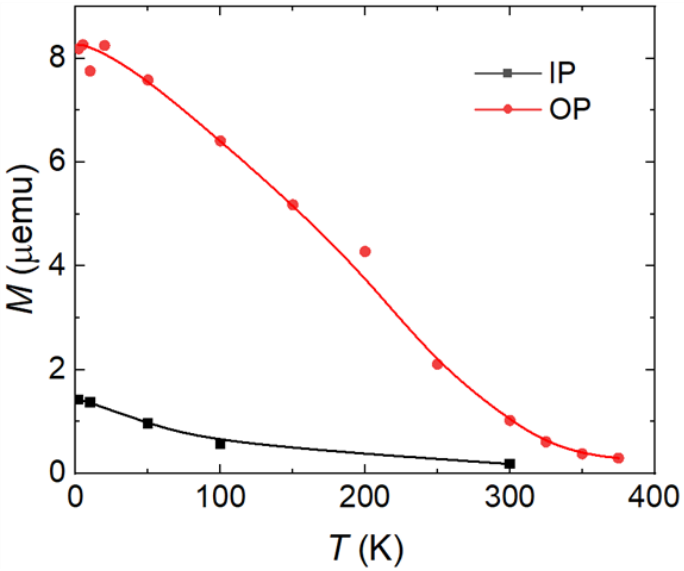

T_C above 350 K

Perpendicular magnetic anisotropy

Lv, … AIF, et al., Small 19, 2302387 (2023)

Comparison with previous works

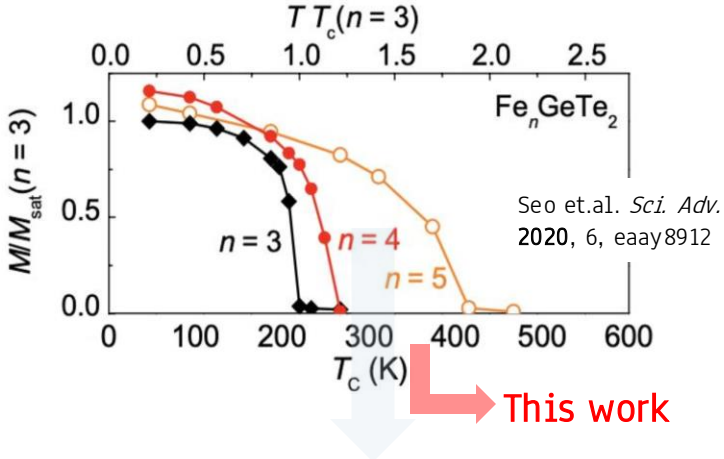

Seo et.al. *Sci. Adv.* **2020**, 6, eaay8912

$Fe_{5-x}GeTe_2$ ($0 < x \leq 0.4$, $T_C \approx 280$ - 320 K)

- May et al., *ACS Nano* **2019**, *13*, 4436 (bulk crystal, flakes)
- Ribeiro, et al., *npj 2D Mater Appl* **2022**, *6*, 10 (MBE film on Al_2O_3)
- Ly et al., *Adv. Funct. Mater.* **2021**, *31*, 2009758 (bulk crystal)
- Nair et al., *Nano Res.* **2022**, *15*, 457. (CSCVD flakes)
- Liu et al. *National Sci. Rev.* **2022**, *9*, nwab117 (MBE film on Al_2O_3)
- Wang, et al., *Nature Comms.* **2023**, 14, 2483 (MBE film on Al_2O_3)

$Fe_{4.75}GeTe_2$ on Gr/SiC

Estimation of T_C and anisotropy from XMCD

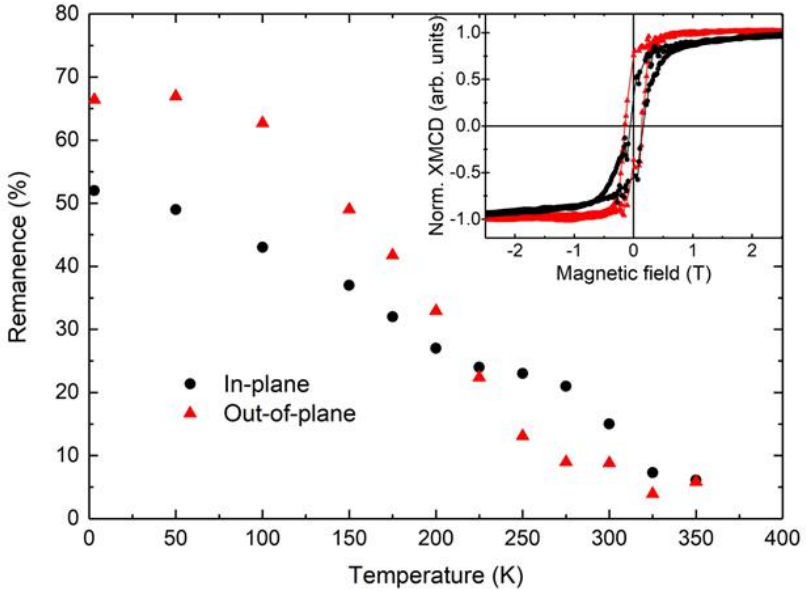

- Ferromagnetic character with T_C above room temperature
- Out-of-plane anisotropy observed at low temperatures
- Magnetization undergoes an in-plane reorientation transition at ~ 220 K
- TEY detection used for XMCD is surface sensitive and probes the topmost FGT layers (~ 5 nm)

Application of sum rules yield an effective magnetic moments

$\mu_{eff} = 1.13 \pm 0.10\ \mu_B$ /Fe

Lv, ... AIF, et al., Small 19, 2302387 (2023)

Fe_3GaTe_2 on Gr/SiC

Macroscopic Magnetometry

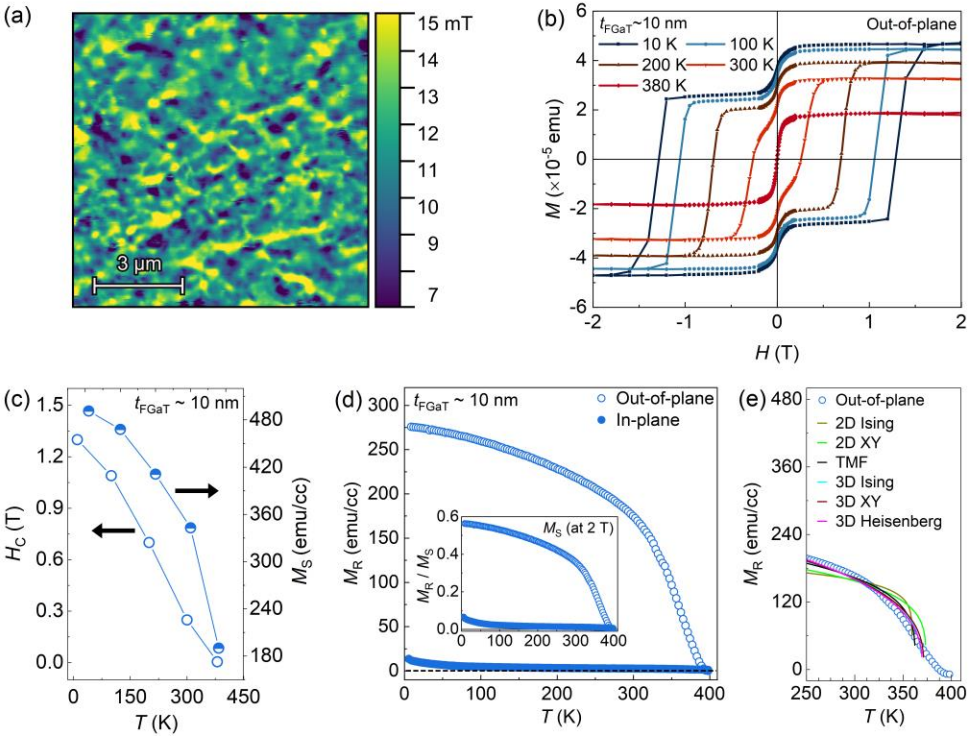

T_C above 380 K

Perpendicular magnetic anisotropy

Critical exponents analysis

$$M_R = M_0\left(1 - \frac{T}{T_C}\right)^{\beta}$$

Best fit using a 3D Heisenberg model: a 10 nm-thick FGaT film already acts as a 3D magnetic system despite a relatively small thickness of only 6 unit cells of FGaT

T. Shinwari1 et al. arXiv:2505.06128v1 (2025)

Fe_3GaTe_2 on Gr/SiC

Magneto-transport

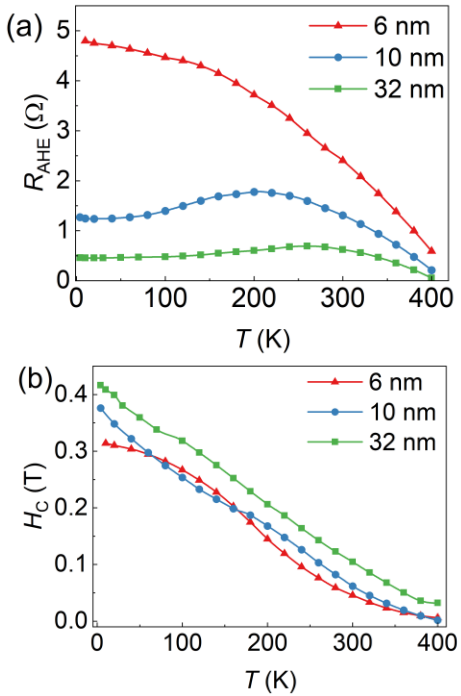

Microscopic Magnetometry: XMCD

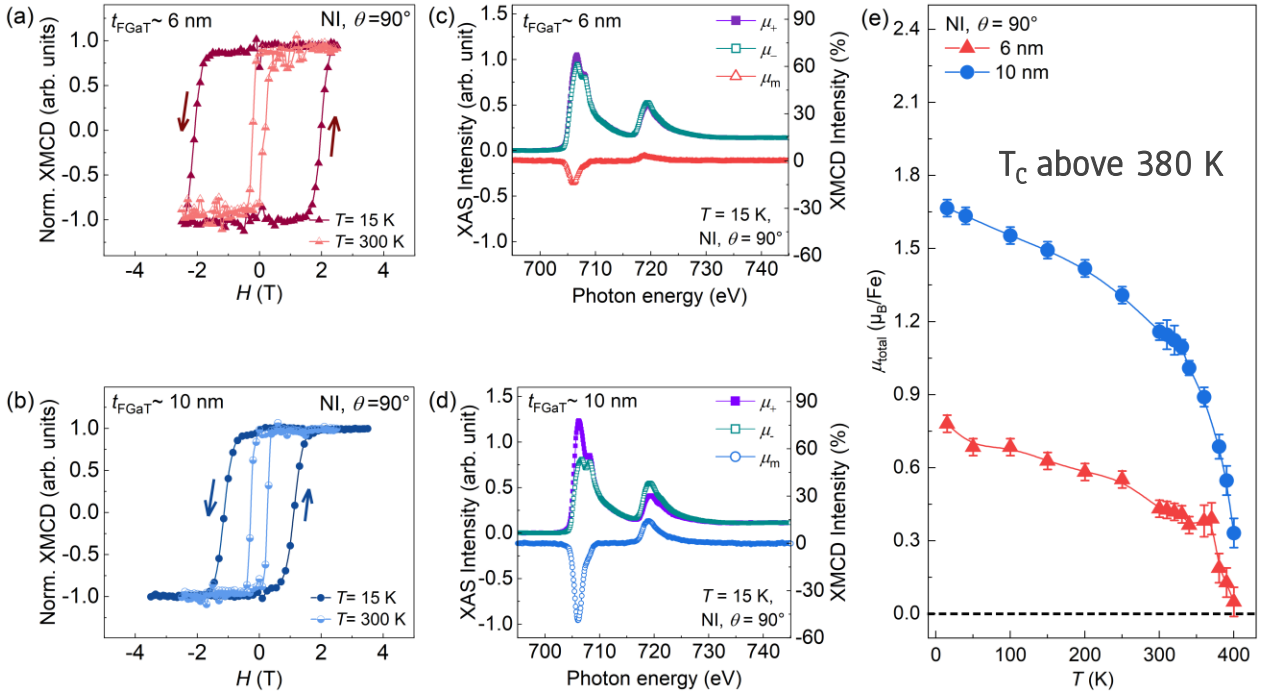

Sum rules analysis: μ_{eff} = 1.16 μ_B /Fe

T. Shinwari1 et al. arXiv:2505.06128v1 (2025)

Conclusions

- XAS and XMCD are powerful SR-based techniques to investigate 2D materials
- High-quality epitaxial growth of vdW heterostructures combining 2D materials: Large area growth of Fe(Ge,Ga)Te and films on graphene by MBE
- Complementary magnetometries, including magneto-transport and XMCD, revealed the macroscopic and microscopic magnetic properties of 2D Fe(Ge,Ga)Te ferromagnets
- Robust perpendicular anisotropy for different Fe concentration
- Composition-dependent TC with values above 350 K for 15 nm $Fe_{4.75}GeTe_2$ and Fe_3GaTe_2 films

THANKS!

Do you have any questions?